DEEPER INSIGHTS

UNVEILING DOPANT PROFILES WITH GIXRD

by

Mark Smith

A senior thesis submitted to the faculty of

Brigham Young University - Idaho

in partial fulfillment of the requirements for the degree of

Bachelor of Science

Department of Physics

Brigham Young University - Idaho

April 2026

BRIGHAM YOUNG UNIVERSITY - IDAHO

DEPARTMENT APPROVAL

of a senior thesis submitted by

Mark Smith

This thesis has been reviewed by the research advisor, research coordinator, and department chair and has been found to be satisfactory.

_____   _____
Date   David Oliphant, Advisor

_____   _____
Date   Jon Johnson, Committee Member

_____   _____
Date   Todd Lines, Committee Member

_____   _____
Date   Todd Lines, Thesis Coordinator

_____   _____
Date   Evan Hansen, Department Chair

ABSTRACT

DEEPER INSIGHTS

UNVEILING DOPANT PROFILES WITH GIXRD

Mark Smith

Department of Physics

Bachelor of Science

In this work, grazing incidence X-ray diffraction (GIXRD) is utilized to investigate the depth profile of dopants in silicon. By systematically varying the X-ray incidence angle, one can precisely control the depth penetrated into doped silicon samples. This approach enables a non-destructive analysis of how dopant concentration evolves with depth. The findings provide crucial insights into the distribution and behavior of dopants, which is essential for optimizing semiconductor device performance and fabrication processes.

ACKNOWLEDGMENTS

Contents

List of Figures

Chapter 1

Background

Solids can be divided into two broad types: crystalline, and amorphous. Crystalline solids have repeating structure that is predictable, and is consistent throughout the entire solid. Amorphous solids have no repeating structures, and have no preferred orientation.

X-Ray diffraction (XRD) utilizes x-rays to non-destructively probe the inner atomic layers of materials. In this work it is used to probe different depths of doped silicon to see dopant levels as a function of depth. As the x-ray interacts with the sample it will reflect, refract, and diffract. Diffraction is the process of note, and the only one that will be investigated for this work.

When XRD is used on crystalline solids a diffraction pattern will emerge. The spacing between the atoms acts as the slit size that allows for the diffraction interference pattern, in accordance with Bragg's Law ($2d \sin \theta = n\lambda$). There also exist different spacings between atoms that are not nearest neighbors. Each of these different spacings are relegated into planes that act like a diffraction grating, existing for every possible repeating spacing within the atom. All of these in superposition produce a graph that shows sharp peaks correlating directly to the atomic plane's
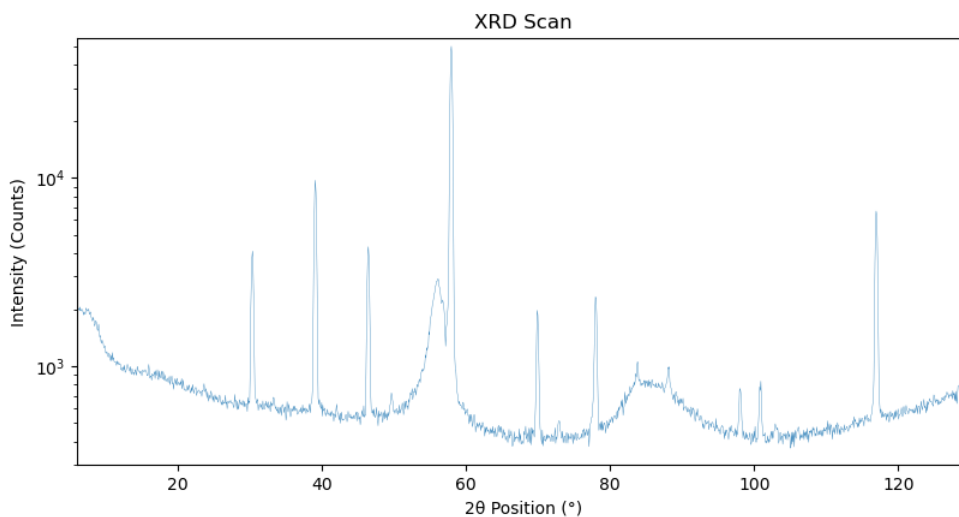
spacing (shown in figure 1.1).

Figure 1.1 Diffractogram of pure crystalline solid

Amorphous solids under the x-ray beam behave in a similar manner. The differ-
ence being because every atom is arranged randomly, there are an infinite number of
planes with their own spacing. As shown in figure 1.2, this correlates to a moderately
low angle hump (called an amorphous hump) with all spacings that would correlate
to higher angled peaks being nonexistent because of deconstructive interference[1–3].
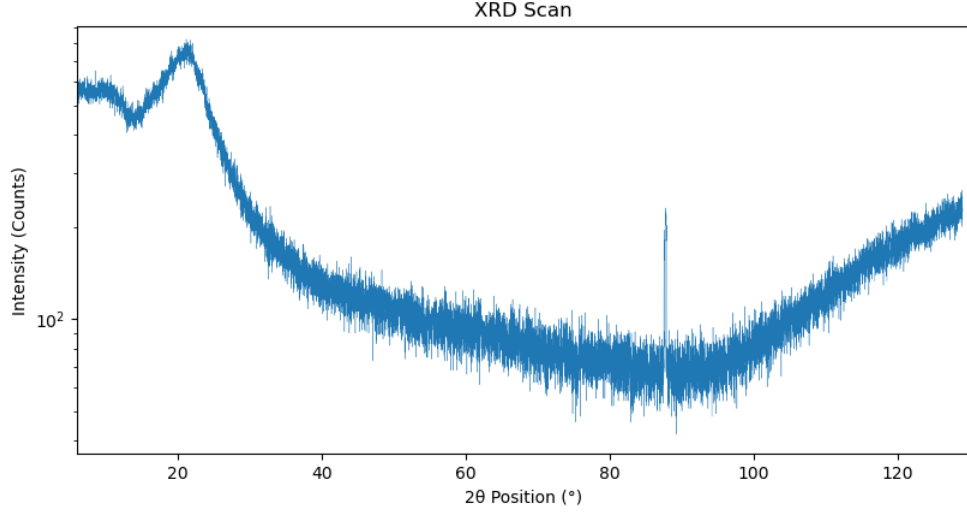
Figure 1.2 Diffractogram of pure amorphous solid

The materials analyzed in this work are silicon doped with phosphorous, silicon doped with boron, and pure silicon. The first two materials will be best thought of as a gradient from pure phosphorous or boron to pure silicon from top to bottom. Silicon is a crystalline material, while phosphorous and boron are amorphous. This means that the diffractogram will be a superposition of an amorphous diffractogram on a crystalline diffractogram. The silicon sample was only used to verify that the amorphous hump was present on the diffractograms.

The different incident angles probe different depths due to the different path lengths they provide the x-rays as they interact with the samples. This is due to the exponential attenuation of intensity as the beam travels given by this equation: $I(y) = I_0 e^{-\alpha y}$ with $\alpha = 2\omega n_I/c$[4, 5]. With the complex index of refraction (n_I) strongly dependent on wavelength. The x-ray source is copper, producing K_α, and K_β in most abundance. Since one wavelength provides the most uniformity on the diffractogram, the incident beam optics include a filter to limit the unnecessary wavelength. K_α is what is most common, so the K_β gets mostly filtered out by a nickel filter. This

results in a x-ray beam that has a wavelength of 1.54Å(uniformity in the wavelength is also necessary for Bragg's law).

Chapter 2

Methods

The process by which the XRD is used in this work to probe increasingly deeper depths is called grazing incidence x-ray diffraction (GIXRD; also called glancing incidence x-ray diffraction). GIXRD holds an incident angle relative to the surface of the sample (called omega (ω)), while the detector on the diffracted beam side sweeps over a range of angles (figure 2.1). The detector is used in 0D mode in conjunction with a parallel plate collimator; This means it simply counts all the x-rays that interact with it. The counts get added to bins according to the current detector angle according to this equation: $2(\omega + \theta)$, with θ being the current detector angle. After the detector has swept through all programed angles, a new scan is started with a different ω corresponding to a different depth.
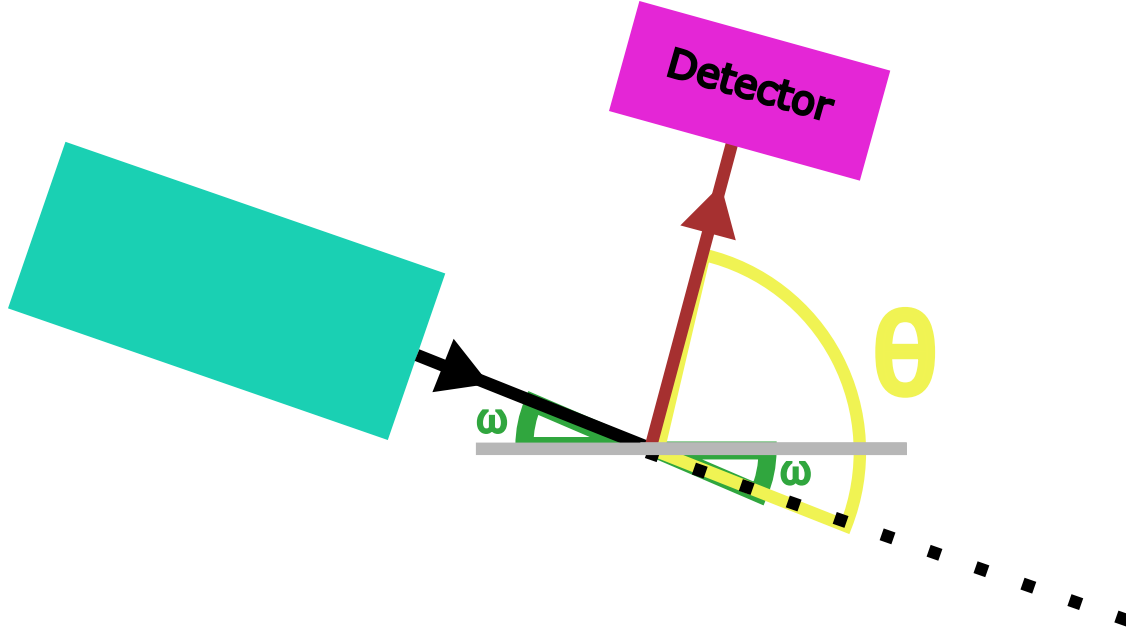
Figure 2.1 Diagram of XRD utilizing GIXRD

Three different methods for determining relative percentages of the dopant in the substrate are used. The methods are named: 1. Intensity, 2. Curve Fitting, and 3. Summation. Before discussing the intricacies of these methods, it is important to first know what shared simplifying assumptions on which they are predicated. The first of these assumptions is that the mixture of the probed depth is uniform. Uniformity of the mixture cannot be achieved in the sample due to the diffusion process starting at the top of the sample working its way down. The next assumption is that the intensity of the x-ray has been attenuated by 90%. The thirdly, that the sample is put in its preferred orientation that allows for the silicon structure to be alined with the x-ray beam. The last assumption is the index of refraction is the same as bulk samples[6] as those values will be utilized.

Method 1: Intensity

This method takes the highest count of the amorphous hump, and the highest count of the crystalline peaks as input parameters, to take the ratio of them. This ratio is then the relative percentages of the dopant and substrate[7]. The following formula is used for the calculation:

$$m = \frac{I_a}{I_a + I_c}$$

I_a is the highest count of the amorphous hump, I_c is the highest count of the crystalline peaks, and m is the mixture percent.

Method 2: Curve Fitting

The amorphous hump, and the crystalline peaks can be approximated by Gaussian curves. As such, it is possible to fit a curve to the hump, and the desired peak. With this fit, analytic integration is performed. The values from the integrations are then taken as a ratio as in the intensity method. This method also gives a background baseline that can be subtracted out.

Method 3: Summation

This method is similar to the curve fitting method, but instead of fitting the hump, and peak to a Gaussian, a numerical integration is performed. This numerical integration sums up the heights in the region of the relevant area to take their ratio. As stated, only the heights are summed; This is due to the spacing between all points being identical. Below is the proof:

$$m = \frac{\sum_{\theta_i}^{\theta_f} y_a dx_a}{\sum_{\theta_i}^{\theta_f} y_a dx_a + \sum_{\theta_i}^{\theta_f} y_c dx_c}$$

$$dx_a = dx_c = Constant$$

$$m = \frac{dx_a \sum_{\theta_i}^{\theta_f} y_a}{dx_a \sum_{\theta_i}^{\theta_f} y_a + dx_c \sum_{\theta_i}^{\theta_f} y_c}$$

$$m = \frac{dx_a \sum_{\theta_i}^{\theta_f} y_a}{dx_a \left(\sum_{\theta_i}^{\theta_f} y_a + \sum_{\theta_i}^{\theta_f} y_c \right)}$$

$$m = \frac{\sum_{\theta_i}^{\theta_f} y_a}{\sum_{\theta_i}^{\theta_f} y_a + \sum_{\theta_i}^{\theta_f} y_c}$$

A similar proof can also be performed to show the counts do not need to be normalized.
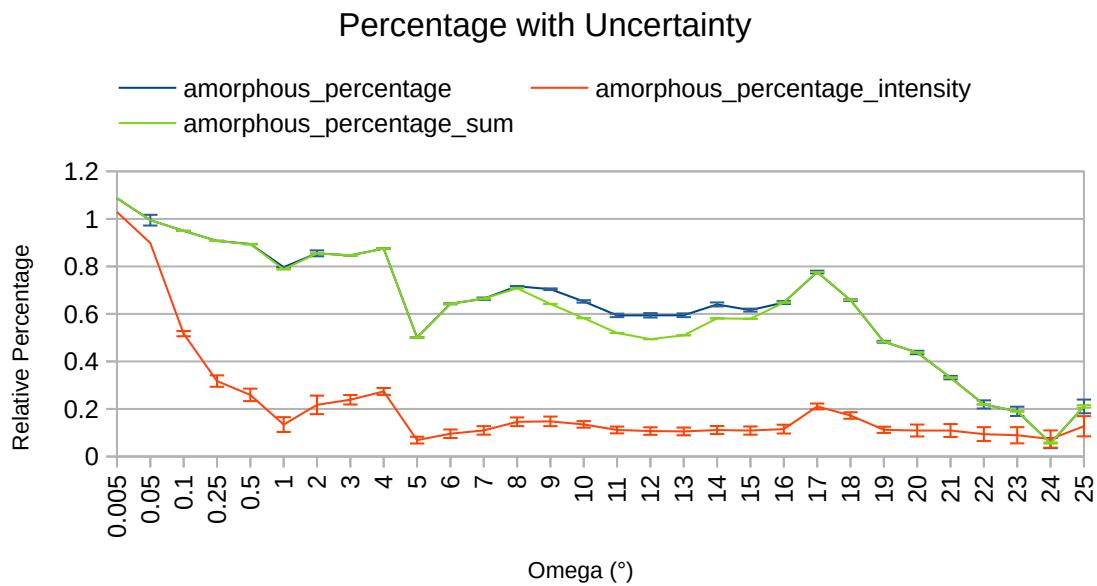
Chapter 3

Results

Percentage with Uncertainty

Figure 3.1 Percentage of amorphous vs omega for the three methods with fractional uncertainty

omega	Intensity	Intensity Fractional Uncertainty	Summation	Summation Fractional Uncertainty
0.005	1.0291		1.0869	
0.05	0.8983	0.0110	0.9946	0.0001
0.1	0.5168	0.0239	0.9495	0.0003
0.25	0.3174	0.0263	0.9070	0.0004
0.5	0.2593	0.0313	0.8936	0.0004
1	0.1344	0.0389	0.7877	0.0008
2	0.2172	0.0197	0.8552	0.0003
3	0.2387	0.0146	0.8467	0.0002
4	0.2737	0.0142	0.8752	0.0002
5	0.0690	0.0181	0.5004	0.0005
6	0.0958	0.0179	0.6426	0.0004
7	0.1098	0.0183	0.6639	0.0004
8	0.1459	0.0203	0.7082	0.0004
9	0.1478	0.0138	0.6417	0.0003
10	0.1351	0.0142	0.5820	0.0004
11	0.1115	0.0157	0.5196	0.0004
12	0.1071	0.0165	0.4938	0.0005
13	0.1056	0.0169	0.5099	0.0005
14	0.1113	0.0173	0.5812	0.0004
15	0.1091	0.0185	0.5794	0.0004
16	0.1153	0.0122	0.6478	0.0003
17	0.2106	0.0136	0.7765	0.0002
18	0.1726	0.0131	0.6580	0.0003
19	0.1123	0.0249	0.4827	0.0008
20	0.1093	0.0273	0.4377	0.0009
21	0.1093	0.0292	0.3320	0.0014
22	0.0942	0.0341	0.2191	0.0021
23	0.0894	0.0364	0.1900	0.0024
24	0.0735	0.0427	0.0564	0.0053
25	0.1273	0.0333	0.2107	0.0025

Figure 3.2 Table for percentage of amorphous vs omega for the three methods with fractional uncertainty
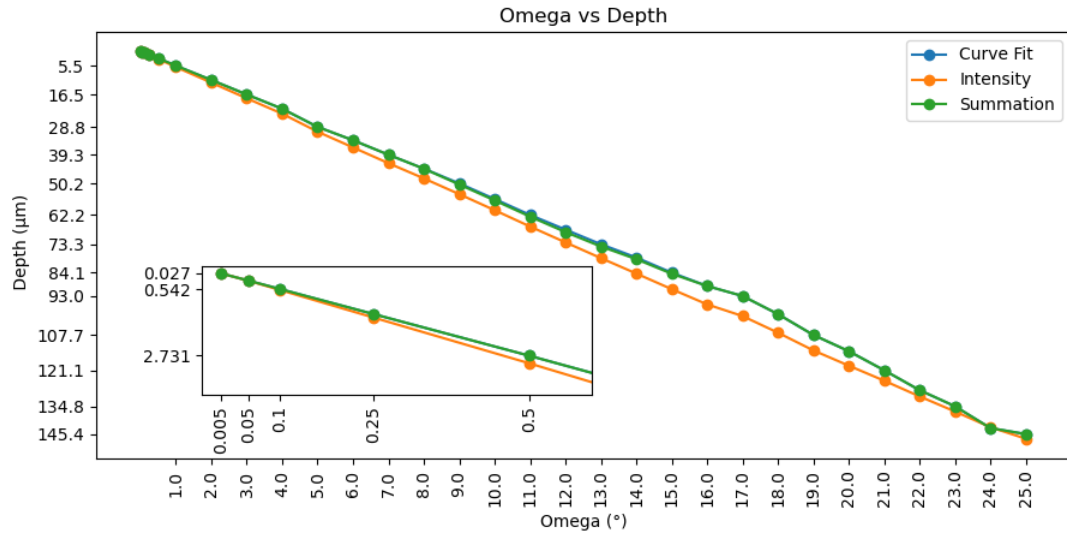

Figure 3.3 Depth vs omega for the three methods

Chapter 4

Analysis

Figure **??** provides a concise overview of how the dopant and substrate mixture change with omega. All three methods show the amorphous percent decreases with depth, which is to be expected. They also show that the 0.005 omega is greater than 1 for the amorphous. This is due to the crystalline peak being nonexistent, but the program is still trying to see a peak. The curve fitting and summation method provide excellent agreement with each other, while the ratio method alludes to an exponential.

Figure 3.3 shows the depth that correlates with the three methods. The methods have a close agreement, with the curve fit and summation method being right on top of each other. They all show a mostly linear relationship, which is to be expected since the indices of refraction are very similar for the dopant and substrate. Nevertheless, it is interesting that the methods more closely agree at lower and high omegas, but not the middle omegas.

Chapter 5

Conclusion

Using GIXRD to determine relative composition of samples led to three analysis methods. Two of the methods utilized integration, and their results are closer alined. One method used peak intensity ratios, and provides results that noticeably differ. All three methods provide reasonable agreement as to the depth that each omega probed. Using GIXRD to see relative mixture amount dependent on depth has been shown to be useful, keeping in mind the limitations given by the assumptions.

5.1   Future Work

Performing this analysis on a known sample would be able to provide greater validity to the results of this analysis. Creating an analysis to correct for the real diffusion process by not assuming uniform layers. This would produce the greatest impact on the real world application of these results.

Bibliography

[1] G. L. Parks, M. L. Pease, A. W. Burns, K. A. Layman, M. E. Bussell, X. Wang, J. Hanson, and J. A. Rodriguez, "Characterization and hydrodesulfurization properties of catalysts derived from amorphous metal-boron materials," Journal of Catalysis **246,** 277–292 (2007).

[2] C. Achilles *et al.*, "AMORPHOUS PHASE CHARACTERIZATION THROUGH X-RAY DIFFRACTION PROFILE MODELING: IMPLICATIONS FOR AMORPHOUS PHASES IN GALE CRATER ROCKS AND SOILS.," In *49th Lunar and Planetary Science Conference 2018 (LPI Contrib. No. 2083)*, 2083 (2018).

[3] A. van Riessen, E. Jamieson, H. Gildenhuys, R. Skane, and J. Allery, "Using XRD to Assess the Strength of Fly-Ash- and Metakaolin-Based Geopolymers," Materials 18 (2025).

[4] J. Liu, R. E. Saw, and Y.-H. Kiang, "Calculation of effective penetration depth in X-ray diffraction for pharmaceutical solids," Journal of Pharmaceutical Sciences **99,** 3807–3814 (2010).

[5] E. Hecht, *Optics*, 4th intern ed. (Addison Wesley, 2002).

[6] P. Colombi, P. Zanola, E. Bontempi, and L. E. Depero, "Modeling of glancing incidence X-ray for depth profiling of thin layers," Spectrochimica Acta Part B: Atomic Spectroscopy **62,** 554–557 (2007), a Collection of Papers Presented at the 18th International Congress on X-Ray Optics and Microanalysis (ICXOM 2005).

[7] A. Pandey, S. Dalal, S. Dutta, and A. Dixit, "Structural characterization of polycrystalline thin films by X-ray diffraction techniques," Journal of Materials Science: Materials in Electronics **32,** 1341–1368 (2021).

Appendix A

XRD Manual

The purpose of an appendix is to provide supplementary information which would distract if included in the main body of the thesis. Items appearing as an appendix might include lengthy derivations. If students feel compelled to include a brief tutorial on relevant background information (not new research), it should appear as an appendix. An appendix might consist of portions of unique computer code that was developed as part of the project.